Automated and Interpretable Experimental Platform for Process-Structure-Property Analysis via Raman Spectroscopy

Takuya Miyajima [1] **Yusaku Nakajima** [1] **Kazuho Saeki** [2] **Masao Yano** [2] **Kanta Ono** [1]

[1]*The University of Osaka, Japan* [2]*Toyota Motor Corporation, Japan.* Correspondence to: Takuya Miyajima takuya_miyajima@ap.eng.osaka-u.ac.jp.

1. Introduction

AM enables the fabrication of complex three-dimensional structures through layer-by-layer processing, its manufacturing processes involve diverse and complex physical phenomena, making it difficult to predict the mechanical properties of fabricated parts solely through simulation[1, 2]. Against this background, the optimization of manufacturing process parameters using automated and autonomous experimental systems has gained attention as an effective approach, with numerous studies reported in recent years. For instance, Gongora et al. combined Bayesian optimization with automated testing in Fused Deposition Modeling (FDM) to optimize structural parameters, discovering high-toughness structures 18 times more efficiently than grid search[3]. However, direct optimization based on process parameters suffers from high device dependency, making it difficult to ensure reproducibility during scale-up or when switching equipment[4, 5, 6].

To address this challenge, we propose using spectral data as a physicochemical intermediate representation between process parameters and mechanical properties. Unlike previous approaches that rely on expert-defined structural features[7], our method concurrently acquires spectroscopic and mechanical data, using machine learning to extract property-relevant features in a data-driven manner.

Here, we apply this methodology to Vat Photopolymerization (VPP), a process favored for high-precision medical and dental applications[8]. In VPP, the printing direction and post-curing critically influence both mechanical and esthetic properties[9, 10]. While post-curing improves strength by increasing crosslink density, it simultaneously affects dimensional accuracy and color[11]. Nevertheless, because complex network microstructures can produce varying mechanical properties even at identical conversion rates, direct process-to-property prediction remains challenging[12].

In this study, we aim to elucidate the process–structure–property relationship in UV-curable methacrylate resins using an automated platform that integrates Raman spectroscopy and tensile testing. A collaborative robot enables continuous, operator-independent analysis of chemical and mechanical properties on the same specimen across varying layer thicknesses and post-curing conditions. This setup captures both monomer conversion and polymer network formation, from which machine learning extracts property-related spectral features. By modeling these features against process parameters, we establish an interpretable framework for understanding how manufacturing conditions dictate final material performance.

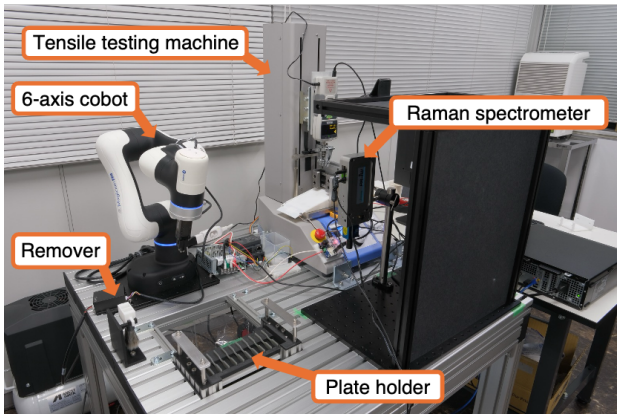

Fig. 1: Overview of the automated experimental platform integrating a 6-axis cobot, a Raman spectrometer, and a tensile testing machine.

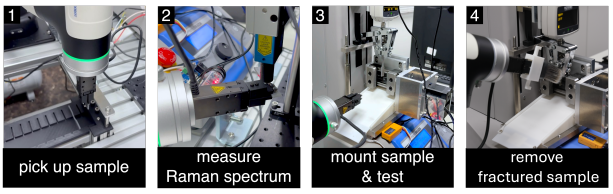

Fig. 2: Measurement workflow: (1) pickup, (2) Raman spectral measurement, (3) specimen mounting and tensile test, and (4) removal of fractured specimen.

2. Method

2.1 Sample Preparation

Specimens were fabricated via stereolithography (Formlabs Form 3) using Draft Resin V2 following JIS K7139. Fifteen conditions ($N = 3$ each) were tested by varying layer thickness (100, 200 μm), post-curing temperature (25, 60 °C), and post-curing time (0, 2, 5, 7, 10 min), with non-cured controls included for each layer thickness.

2.2 Automated Experimental Platform

2.2.1 System Configuration

As shown in Fig. 1, the automated experimental system consists of a 6-axis robotic arm integrated with sample holders (10 samples per plate, 9 plates maximum), a gripping unit, and a fractured specimen removal mechanism. Raman spectra were acquired using a palmtop Raman spectrometer (JASCO

PR-1w), and tensile testing was performed using a force gauge with measurement stand (Imada ZTS-500N, MX2-2500N).

2.2.2 *Automated Workflow*

The workflow begins with defining process parameters (layer thickness, post-curing time and temperature), followed by fabrication of UV-cured specimens. Raman spectroscopy and tensile testing are then performed on each specimen (Fig. 2), with all data automatically recorded in a database.

2.3 *Machine Learning Framework*

Spectral-Based Property Prediction PLS regression with Target Projection (TP) [13] was applied to predict mechanical properties from Raman spectra, reducing spectral information to TP scores. The Selectivity Ratio (SR) provides quantitative identification of wavenumber regions contributing to strength beyond what is apparent from visual spectral analysis, with the sign indicating positive or negative correlation.

Process-to-Spectrum Modeling To predict TP scores from process parameters (layer thickness, post-curing time, and temperature), we employed Random Forest (RF) regression. RF was selected for its ability to capture non-linear interactions between parameters while maintaining interpretability through SHAP values[14].

Integrated Analysis Framework By integrating the above analytical methods, we established a framework to systematically solve the forward problem of how process conditions alter the spectra and how those spectral changes affect the mechanical properties. Specifically, this allows for tracking the information flow from Process Parameters → TP Scores → SR Analysis → Mechanical Properties.

3. Results and Discussion

3.1 *Spectral-Based Prediction of Mechanical Properties*

Following the automated workflow, Raman spectroscopy (2 s integration, 5 accumulations) and tensile testing (10 mm/min) were performed to measure UTS.

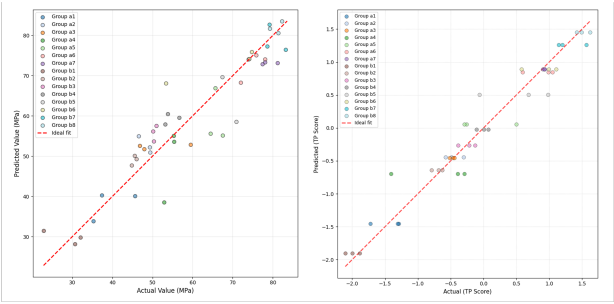

Fig. 3: Two-stage modeling performance for UTS prediction. Left: PLS regression predicting UTS from spectra. Right: Random Forest regression predicting TP scores from process parameters. Each color represents a different process condition group.

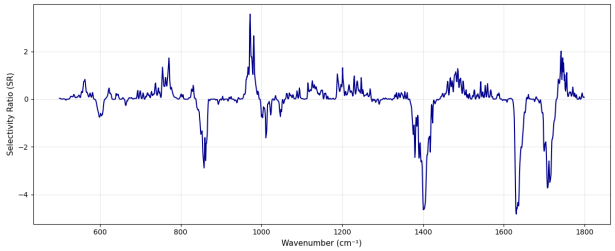

Fig. 4: Selectivity Ratio (SR) plot highlighting Raman bands contributing to UTS prediction. Positive/negative values indicate wavenumbers positively/negatively correlated with UTS.

PLS regression with two latent variables achieved high predictive accuracy (R^2 = 0.86, LOCO-CV Q^2 = 0.70) (Fig. 3), demonstrating that Raman spectra effectively capture mechanical property determinants. Figure 4 shows the corresponding Selectivity Ratio (SR) plot, highlighting key spectral features: reduction of unreacted monomers (810, 1400, 1640, 1740 cm^{-1}) and increase in polymer network formation (970 cm^{-1}) contribute to strength improvement.

3.2 *Process–Structure–Property Relationship*

Random Forest regression predicted TP scores from process parameters with R^2 = 0.95 (LOCO-CV Q^2 = 0.76). Feature importance analysis revealed post-curing temperature as the dominant factor (SHAP: 0.67), followed by post-curing time (0.34) and layer thickness (0.13). This two-stage modeling automatically identified structure-property relationships in a data-driven manner, enabling physicochemical interpretation of optimal conditions.

3.3 *Limitations*

The residual 13% unexplained variance likely reflects internal structural heterogeneity beyond Raman's surface-probing depth. While effective for elastic properties, this approach may be less suitable for highly ductile materials where dynamic fracture mechanisms dominate.

4. Conclusions

We proposed a two-stage modeling approach using Raman spectroscopy as a physicochemical intermediate between process parameters and mechanical properties in stereolithography. This framework provides three key advantages: (1) device-independent knowledge transfer through spectroscopic descriptors that directly reflect chemical structure (polymerization degree, crosslink density), (2) automated, data-driven identification of property-relevant structural features without prior expert knowledge, and (3) transferability to other photocurable systems. Future work will integrate Raman spectra within Bayesian optimization frameworks for efficient, non-destructive process optimization.

Acknowledgements

This work was partly supported by Toyota Motor Corporation, the JST-Mirai Program (Grant Number JPMJMI21G2).

Appendix A: Preprocessing and Model Configuration

A.1 Data Exclusion

Samples post-cured at 60°C for 10 min were tested but excluded from the training dataset, as their tensile strength exceeded the apparatus measurement limit.

A.2 Raman Spectral Preprocessing

All Raman spectra were preprocessed using RamanSPy [15] with the following sequential steps:

1. Despiking: Whitaker-Hayes algorithm
2. Smoothing: Savitzky-Golay filter (window size: 7, polynomial order: 3)
3. Baseline correction: Adaptive iteratively reweighted penalized least squares (airPLS)
4. Normalization: Standard normal variate (SNV) transformation

A.3 PLS Regression Configuration

- Number of latent variables: 2
- Cross-validation: Leave-one-condition-out (LOCO-CV)

A.4 Random Forest Configuration

- Number of trees: 484
- Mean max depth: 5.2
- Mean leaf nodes: 13.2
- Hyperparameter optimization: Random search with cross-validation

References

[1] S. Garzon-Hernandez, D. Garcia-Gonzalez, A. Jérusalem, and A. Arias. Design of fdm 3d printed polymers: An experimental-modelling methodology for the prediction of mechanical properties. *Materials & Design*, 188:108414, 2020.

[2] S. Westbeek, J.J.C. Remmers, J.A.W. van Dommelen, H.H. Maalderink, and M.G.D. Geers. Prediction of the deformed geometry of vat photopolymerized components using a multi-physical modeling framework. *Additive Manufacturing*, 40:101922, 2021.

[3] Aldair E. Gongora, Bowen Xu, Wyatt Perry, Chika Okoye, Patrick Riley, Kristofer G. Reyes, Elise F. Morgan, and Keith A. Brown. A bayesian experimental autonomous researcher for mechanical design. *Science Advances*, 6(15):eaaz1708, 2020.

[4] Ersilia Cozzolino, Gabriela Del Risco, Natalia von Windheim, Cameron Gygi, Antonello Astarita, and Nathan Ames. Scaling up the 3d printing of surgical guides: repeatability and energy efficiency. *Rapid Prototyping Journal*, 31(11):148–159, 03 2025.

[5] Davis J. McGregor, Miles V. Bimrose, Chenhui Shao, Sameh Tawfick, and William P. King. Using machine learning to predict dimensions and qualify diverse part designs across multiple additive machines and materials. *Additive Manufacturing*, 55:102848, 2022.

[6] K. Ouajjani, J.E. Steck, and G. Olivares. Leveraging machine learning for porosity prediction in AM using FDM for pretrained models and process development. *Materials*, 18(19):4499, 2025.

[7] Yoshiki Sakai, Kota Aono, Takayuki Osa, Moju Zhao, Hirotoshi Tagata, Masanori Nakano, Akio Suguro, Masayuki Nakao, and Keisuke Nagato. Autonomous parameter exploration in thermoplastic material-extrusion additive manufacturing using Bayesian optimization with intermediate features. *Journal of Manufacturing Processes*, 157:798–807, 2026.

[8] Ans Al Rashid, Waqas Ahmed, Muhammad Yasir Khalid, and Muammer Koç. Vat photopolymerization of polymers and polymer composites: Processes and applications. *Additive Manufacturing*, 47:102279, 2021.

[9] Yifan Li and Zhenjie Teng. Effect of printing orientation on mechanical properties of SLA 3D-printed photopolymer. *Fatigue & Fracture of Engineering Materials & Structures*, 47(5):1531–1545, 2024.

[10] C. Espinar, A.D. Bona, M.M. Pérez, M. Tejada-Casado, and R. Pulgar. The influence of printing angle on color and translucency of 3D printed resins for dental restorations. *Dental Materials*, 39(4):410–417, April 2023.

[11] J. Soto-Montero, E.F. de Castro, B.C. Romano, G. Nima, C.A.K. Shimokawa, and M. Giannini. Color alterations, flexural strength, and microhardness of 3D printed resins for fixed provisional restoration using different post-curing times. *Dental Materials*, 38(8):1271–1282, August 2022.

[12] R. Anastasio, W. Peerbooms, R. Cardinaels, and L. C. A. van Breemen. Characterization of ultraviolet-cured methacrylate networks: From photopolymerization to ultimate mechanical properties. *Macromolecules*, 52(23):9220–9231, 2019.

[13] Olav M. Kvalheim. Interpretation of partial least squares regression models by means of target projection and selectivity ratio plots. *Journal of Chemometrics*, 24(7-8):496–504, 2010.

[14] Scott Lundberg and Su-In Lee. A unified approach to interpreting model predictions, 2017.

[15] Dimitar Georgiev, Simon Vilms Pedersen, Ruoxiao Xie, Álvaro Fernández-Galiana, Molly M. Stevens, and Mauricio Barahona. RamanSPy: An open-source Python package for integrative Raman spectroscopy data analysis. *Analytical Chemistry*, 96(21):8492–8500, 2024.